Low-Energy Electronic Structure of the Kondo Insulator YbB_{12}

T. Susaki,[1] A. Sekiyama,[1] K. Kobayashi,[1] T. Mizokawa,[1] A. Fujimori,[1] M. Tsunekawa,[2] T. Muro,[2] T. Matsushita,[2,*] S. Suga,[2] H. Ishii,[3] T. Hanyu,[3] A. Kimura,[4] H. Namatame,[5] M. Taniguchi,[5] T. Miyahara,[6] F. Iga,[5] M. Kasaya,[7] and H. Harima[8]

[1]*Department of Physics, University of Tokyo, Bunkyo-ku, Tokyo 113, Japan*
[2]*Department of Material Physics, Osaka University, Toyonaka, Osaka 560, Japan*
[2]*Department of Physics, Tokyo Metropolitan University, Hachioji, Tokyo 192-03, Japan*
[4]*Institute for Solid State Physics, University of Tokyo, Roppongi, Minato-ku, Tokyo 106, Japan*
[5]*Department of Materials Sciences, Hiroshima University, Higashi-Hiroshima 739, Japan*
[6]*Photon Factory, National Laboratory for High Energy Physics, Tsukuba, Ibaraki 305, Japan*
[7]*Department of Physics, Tohoku University, Sendai 980-77, Japan*
[8]*College of Integrated Arts and Science, University of Osaka Prefecture, Gakuen-cho, Sakai 593, Japan*

(Received 20 May 1996; revised manuscript received 31 July 1996)

We have studied the low-energy electronic structure of a Kondo insulator YbB_{12} by high-resolution photoemission spectroscopy. A "Kondo peak" is observed $\sim$25 meV below the Fermi level, which agrees well with the Kondo temperature, whereas the gap at the Fermi level is found much smaller, indicating that the magnetic properties at higher temperatures ($\lesssim$75 K) are indeed determined by the Kondo effect in spite of the gap formation at lower temperatures. A renormalized band picture is presented to describe the coexistence of the Kondo peak and the transport gap as well as the highly asymmetric line shape of the Kondo peak. [S0031-9007(96)01690-0]

PACS numbers: 79.60.Bm, 71.28.+d, 75.30.Mb

Correlated electron systems have fascinated researchers for decades not only because of their interesting ground-state and excited-state properties themselves but also because of their intermediate nature between the localized and itinerant limits, which often requires a new description of the phenomena or even a new physical concept. A class of f-electron compounds termed "Kondo insulators" have attracted considerable interest in recent years [1]: They are nonmagnetic insulators at low temperatures and behave as local-moment (and often metallic) systems at high temperatures. It has been controversial whether the insulating gaps are due to Kondo interaction of local character [2] or they are hybridization gaps renormalized by electron correlation [3]. In the former case, a local description of the electronic structure should be more appropriate and the single-site Kondo temperature T_K would set the energy scale of low-energy physics [4]. In the latter case, an itinerant picture or band theory, which explicitly treats the lattice periodicity, would provide a relevant starting point. It is therefore of essential importance to obtain experimental information about the low-energy electronic structure of the Kondo insulators.

In this Letter we report on a high-resolution photoemission spectroscopy (PES) study of YbB_{12}, which is the only Kondo insulator among various Yb compounds [5–7]. Its magnetic susceptibility shows a Curie-Weiss behavior above $\sim$170 K; as the temperature decreases, it shows a broad maximum at $\sim$75 K and then rapidly decreases. The electrical resistivity and the electronic specific heat are explained by the opening of a transport gap $\Delta_c \sim$130 K [5,6]. Among Kondo systems, Yb compounds are suitable to the study of their low-energy electronic structures by PES because within the framework of the Anderson-impurity model (AIM), a Kondo peak is predicted to appear below the Fermi level (E_F) [8,9] and can therefore be studied with high-energy resolution. Recent PES studies have indeed indicated the existence of the Kondo peak in some metallic Yb compounds [10,11]. Our results have also revealed a Kondo peak $\sim$25 meV below E_F, indicating that the same picture properly describes the Kondo insulator YbB_{12} on this energy scale. The insulating behavior manifests itself on a smaller energy scale as a much smaller gap at E_F. In order to describe the coexistence of the Kondo peak and the tiny gap as well as the strongly asymmetric line shape of the Kondo peak, we have employed a phenomenological renormalized f-band picture, starting from the band structure calculated by means of the local-density approximation (LDA) [12].

Polycrystalline samples of YbB_{12} were prepared by borothermal reduction at 2200 °C and were checked to be in a single phase by x-ray diffraction. A small amount ($\sim$3%) of Lu was substituted for Yb to obtain good quality samples. Their magnetic susceptibility and the electrical resistivity are almost identical to those of pure YbB_{12} at least for $T > 20$ K [7]. The Lu-substitution introduces n-type carriers into the semiconducting samples, but the conductivity is rather intrinsic above $\sim$20 K and the Fermi level is supposed to be located in the middle of the $\sim$130 K semiconducting gap.

Ultraviolet PES measurements were performed with the He I and He II resonance lines ($h\nu = 21.2$ and 40.8 eV, respectively) as well as synchrotron radiation at BL-3B of the Photon Factory, National Laboratory for High Energy

Physics. A VSW CLASS-150 analyzer and a SCIENTA SES-200 analyzer were used for energy analysis. Energy calibration and estimation of the instrumental resolution were done for a Au film evaporated on the surface of the samples after each series of measurements. The resolution was 23, 42, and ~55 meV for the He I, He II, and synchrotron radiation measurements, respectively. All measurements were done at 30 ± 5 K. The base pressure of the spectrometer was $\sim 7 \times 10^{-11}$ Torr for the He I and He II measurements and $\sim 4 \times 10^{-10}$ Torr for the synchrotron radiation measurements. The surface of the samples was repeatedly scraped *in situ* with a diamond file.

Figure 1(a) shows the valence-band spectrum taken with the photon energy of 125 eV, for which the Yb $4f$ contribution is dominant [13]. The spectral features in the range from 4 to 13 eV are assigned to the $4f^{13} \rightarrow 4f^{12}$ multiplet structure [14]. Between E_F and 4 eV are observed $4f^{14} \rightarrow 4f^{13}$ transitions. As shown in Fig. 1(b), they consist of two sets of $4f^{13}$ spin-orbit doublets. The sharper doublet closer to E_F originates from Yb atoms in the bulk and the broader one away from E_F from divalent Yb atoms on the surface [9,10]. The surface and bulk signals are represented by Gaussians and Mahan's asymmetric line shapes [15], respectively, as shown in the figure. The Yb valence in the bulk estimated from the intensity ratio of the $4f^{13} \rightarrow 4f^{12}$ and $4f^{14} \rightarrow 4f^{13}$ signals is 2.86 ± 0.06, i.e., the number of $4f$ holes $n_f = 0.86 \pm 0.06$, in good agreement with the value 0.85 deduced from the high-temperature magnetic susceptibility [16].

Figure 2 shows the spectra near E_F taken with various photon energies. According to the photoionization cross-sections [13], the He I spectrum (a) is dominated by the B $2p$ contribution. In the He II spectrum (b), a weak Yb $4f$ contribution is also present as an additional intensity within ~0.2 eV of E_F. To extract the Yb $4f$ contribution, we have subtracted the He I spectrum from the He II spectrum and obtained a quite asymmetric peak as shown in Fig. 2(d). This line shape agrees with the 125 eV spectrum (c), except for the differences due to the energy resolution and small boron contribution in the 125 eV spectrum (there is uncertainty in the region >0.3 eV, where the surface signals overlap). By fitting the f-derived spectrum using Mahan's line shape convoluted with a Gaussian which represents the instrumental resolution and then removing the Gaussian convolution, we find that the peak position is ~25 meV below E_F, as shown by the dashed curve in Fig. 2(d).

First, we discuss the spectrum near E_F within the framework of the AIM [8]. In a metallic system, the Kondo temperature T_K, defined as the binding energy of the Kondo singlet, is estimated through $T_K \sim 3T_{\max}$, where $T_{\max}$ is the temperature at which the susceptibility shows a maximum [17], or through $T_K = Cn_f/\chi(0)$, where $C = 2.57$ emuK/mole is the Curie constant of the Yb^{3+} ion and $\chi(0)$ is the magnetic susceptibility at $T = 0$ K. In YbB_{12}, since $\chi(T)$ drops below $T \sim 75$ K due to the gap formation, we have assumed that $\chi(0)$ would take a value comparable to $\chi(T_{\max}) = 1.0 \times 10^{-2}$ emu/mole [5] if the gap was not opened. Both estimations give $T_K \sim 220$ K. According to the AIM, the position of the Kondo peak ε_f measured from E_F is equal to $k_B T_K$ in a metallic system [17], as has been confirmed experimentally for $YbAl_3$ [10]. In the case of YbB_{12}, too, $k_B T_K \sim 19$ meV is in good agreement with the experimental result of $\varepsilon_f \sim 25$ meV. Therefore it seems that the Kondo effect is present both for the metallic and insulating Yb compounds in the photoemission spectra and in the magnetic susceptibility above $T \sim T_{\max}$.

The insulating nature of YbB_{12} is reflected on the He I spectrum (Fig. 3), which is dominated by the B p contribution. From comparison with the Fermi edge of Au in the figure, one identifies the opening of a gap or a pseudogap at E_F. In the intrinsic conduction regime, the

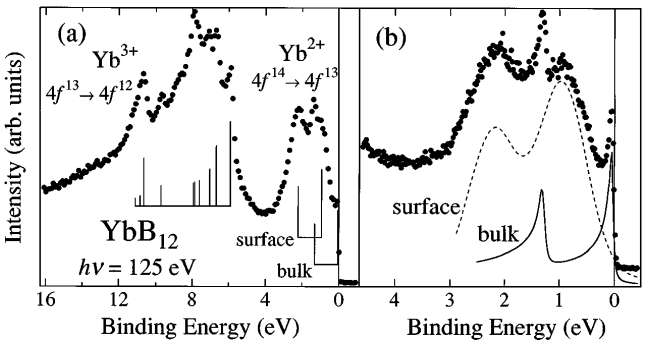

FIG. 1. (a) Valence-band spectrum of YbB_{12} in a wide energy range. For the $4f^{13} \longrightarrow 4f^{12}$ part, the calculated multiplet structure [14] is also shown. (b) $4f^{14} \longrightarrow 4f^{13}$ part of the spectrum. The solid and dashed curves represent signals from the bulk and surface Yb atoms, respectively.

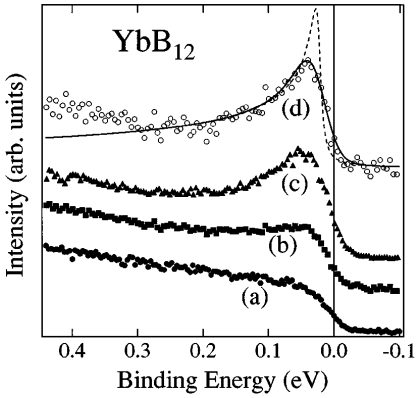

FIG. 2. Spectra near E_F for photon energies of 21.2 eV (a), 40.8 eV (b), and 125 eV (c). (d) is the (b)-(c) difference spectrum, representing the $4f$-derived spectrum. The solid curve is a fit using Mahan's line shape convoluted with a Gaussian representing the instrumental resolution. The dashed curve is the same curve but without the convolution.

top of the occupied valence band should be separated from E_F by the transport activation energy $E_{\rm act} \simeq \frac{1}{2}\Delta_c \sim 6$ meV [5]. From Fig. 3 one can say that the top of the valence band is at E_F or at most several meV below it, due to the limited resolution of 23 meV. According to the band-structure calculation, YbB_{12} is a semimetal [18]. Since LDA underestimates band gaps [19], we have rigidly shifted the valence and conduction bands towards the opposite directions by hand in order to open a finite band gap and to compare the calculated density of states (DOS) with the photoemission spectra as shown in Fig. 3. The observed band edge is thus found to be much steeper than the calculated B p partial DOS, indicating strong renormalization (i.e., narrowing) of energy bands near E_F. Since B sp states themselves are not expected to be strongly correlated, the Yb $4f$ components hybridizing with the B sp states should have caused the strong renormalization. A similar picture has been corroborated by an exact diagonalization study of the Anderson lattice as a model for a Kondo insulator [20].

Therefore we expect that the Yb $4f$ spectral line shape is likewise subject to the strong renormalization of energy bands. Instead of first-principles approaches such as second-order perturbation calculations [21], we have employed a phenomenological approach and fitted the observed spectral line shape using a model self-energy correction. As shown in Fig. 4 by the dashed curve, the Yb f partial DOS has structures from ~150 to ~400 meV while the observed peak position is ~40 meV below E_F. This peak exhibits a steep rise from E_F as in the case of the B $2p$-derived He I spectrum, and a slow tailing off on the higher binding energy side, resulting in a highly asymmetric line shape. This indicates that the band narrowing is energy dependent and is stronger near E_F. The model self-energy which we have employed to calculate the $4f$ spectral function $\rho_f(\omega)$ is of the same type as that previously used for FeSi [12]:

$$\Sigma(\omega) = \Sigma_h(\omega) + \Sigma_l(\omega) + \Sigma_{l'}(\omega), \qquad (1)$$

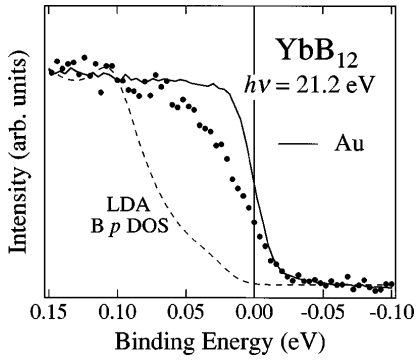

FIG. 3. He I spectrum of YbB_{12} in the vicinity of E_F. The solid curve is the spectrum of Au evaporated onto the sample. The B p partial DOS given by the LDA band-structure calculation broadened by the instrumental resolution is also shown.

where

$$\Sigma_h(\omega) = \frac{g_h(\omega - \delta)}{(\omega - \delta + i\gamma_h)^2},$$

$$\Sigma_j(\omega) = -g_j\left(\frac{1}{\omega - \delta + i\gamma_j} + \frac{i}{\gamma_j}\right) \qquad (j = l, l').$$

Here $-\omega$ is the binding energy measured from E_F and $\omega = \delta \sim -5$ meV is the top of the valence band estimated from the leading-edge shift of the He I spectrum. Equation (1) satisfies the Kramers-Kronig (KK) relation and behaves as $\Sigma(\omega) \sim -a(\omega - \delta) - ib(\omega - \delta)^2$ for small $|\omega - \delta|$ as in a Fermi liquid. For simplicity, we have neglected the momentum-dependence of the self-energy [21,22]. The spectrum could be best reproduced with $g_h = 24.0\ \text{eV}^2$, $\gamma_h = 4.0$ eV, $g_l = 0.025\ \text{eV}^2$, $\gamma_l = 0.08$ eV, $g_{l'} = 0.0015\ \text{eV}^2$, and $\gamma_{l'} = 0.015$ eV as shown in Fig. 4. The high-energy-scale component $\Sigma_h(\omega)$ causes the shift of the structure between ~0.1 and ~0.25 eV in the LDA DOS to the Kondo peak (at ~25 meV below E_F after having removed the Gaussian broadening) and the shift of the structure around ~0.3 eV in the LDA DOS to the higher binding energy side of the peak. The low-energy-scale components $\Sigma_l(\omega)$ and $\Sigma_{l'}(\omega)$ were necessary to reproduce the steep rise in the vicinity of E_F. As a result the negative slope of $\text{Re}\Sigma(\omega)$ increases as one approaches E_F. This in turn increases $|\text{Im}\Sigma(\omega)|$ away from E_F through the KK relation, which explains how the DOS peak at ~0.3 eV in the LDA is smeared out and results in the asymmetric single peak in the measured spectrum. The resulting $|\text{Im}\Sigma(\omega)|$ shows a V-shaped line shape near E_F, a remi-

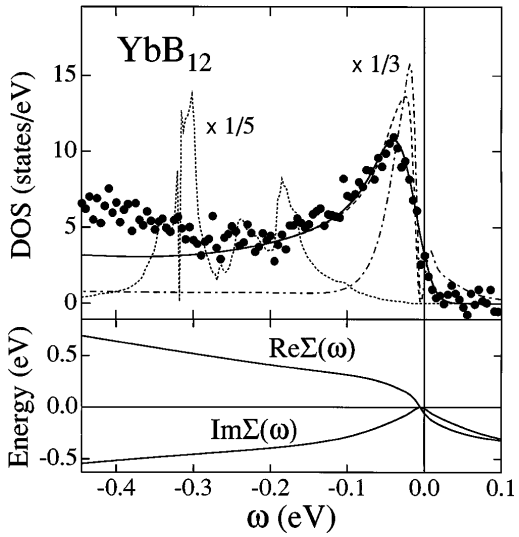

FIG. 4. Yb $4f$ spectrum of YbB_{12} (dots), the Yb f partial DOS (dashed curve), the calculated spectral function $\rho_f(\omega)$ with and without the instrumental broadening (solid curve and long dashed curve, respectively), and the quasi-particle DOS $N^*(\omega)$ (dot-dashed curve). The self-energy $\Sigma(\omega)$ used to calculate the spectral function is shown in the lower panel.

niscent behavior of the marginal Fermi liquid proposed by Varma *et al.* [23]. In Fig. 4 the quasi-particle DOS $N^*(\omega) \equiv \rho_f(\omega)[1 - \partial \mathrm{Re}\,\Sigma(\omega)/\partial\omega]$ is also plotted by the dot-dashed curve.

To establish the relationship between the Kondo effect and the formation of the semiconducting gap on microscopic grounds is beyond the scope of the present phenomenological approach. In the renormalized band picture, the Kondo peak and the semiconducting gap are influenced by the different regions of the self-energy with different slopes $\partial \mathrm{Re}\,\Sigma(\omega)/\partial\omega$. However, this does not exclude the possibility that the disappearance of the local moment and that of spectral weight at $\omega \sim 0$ in the optical conductivity show parallel temperature dependence as in $Ce_3Bi_4Pt_3$ [2] because the electrical conductivity and the magnetic susceptibility have characteristic temperatures of similar magnitudes: $E_{\mathrm{act}}/k_B \sim T_{\mathrm{max}}$. In the local description of the Kondo insulator by Kasuya [4], the Yb $4f$ hole forms a singlet bound state with a conduction electron, the binding energy being given by $k_B T_K$. The local Kondo picture and the renormalized f-band picture should be complementary to each other, describing the different phenomena of the same correlated insulator starting from the different, i.e., localized and itinerant, limits. How the transport gap and the Kondo peak change with temperature or with electron doping (in $Yb_{1-x}Lu_xB_{12}$) studied by PES would give further valuable information about the gap formation. Direct observation of quasi-particle dispersions using a single crystal by angle-resolved PES is also an important future subject. Finally, we remark that the strong energy dependence of mass renormalization may not be unique to the Kondo insulators but may be a general phenomenon in valence-fluctuating f-electron systems because strong asymmetry has also been reported for metallic $YbAgCu_4$ [11] and $YbAl_3$ [9].

To summarize, we have studied the low-energy electronic structure of YbB_{12} using high-resolution PES. The observed position of the Kondo peak agrees well with the Kondo temperature estimated from the magnetic susceptibility above $T \sim T_{\mathrm{max}}$, indicating that single-site Kondo effect indeed governs the magnetic properties in this temperature range in spite of the presence of the transport gap of $\Delta_c \sim 130$ K. The coexistence of the Kondo peak and the transport gap has been described in the phenomenological renormalized band picture. The mass renormalization is thus shown to be strongly energy dependent near E_F, leading to the highly asymmetric Kondo peak.

The authors would like to thank S-.J. Oh, K. Ueda, T. Saso, and T. Kasuya for useful comments and suggestions and the staff of the Photon Factory for valuable technical support. This work has been approved by the Photon Factory Program Advisory Committee (92S002). Financial support from the New Energy and Industrial Technology Development Organization (NEDO) is also acknowledged.

*Present address: Photon Factory, National Laboratory for High Energy Physics, Tsukuba, Ibaraki 305, Japan.

[1] G. Aeppli and Z. Fisk, Comments Condens. Matter Phys. **16**, 155 (1992).
[2] B. Bucher, Z. Schlesinger, P. C. Canfield, and Z. Fisk, Phys. Rev. Lett. **72**, 522 (1994).
[3] N. F. Mott, Philos. Mag. **30**, 403 (1974).
[4] T. Kasuya, Europhys. Lett. **26**, 277 (1994).
[5] M. Kasaya, F. Iga, M. Takegahara, and T. Kasuya, J. Magn. Magn. Mater. **47–48**, 429 (1985).
[6] F. Iga, M. Kasaya, and T. Kasuya, J. Magn. Magn. Mater. **76–77**, 156 (1988).
[7] F. Iga, M. Kasaya, and T. Kasuya, J. Magn. Magn. Mater. **52**, 279 (1985).
[8] O. Gunnarsson and K. Schönhammer, Phys. Rev. B **28**, 4315 (1983).
[9] S.-J. Oh *et al.*, Phys. Rev. B **37**, 2861 (1988).
[10] L. H. Tjeng *et al.*, Phys. Rev. Lett. **71**, 1419 (1993); A. P. Murani, *ibid.* **72**, 4153 (1994).
[11] P. Weibel *et al.*, Z. Phys. B **91**, 337 (1993). Discrepancy between the Kondo temperature T_K and the Kondo peak position ε_f reported for $YbAgCu_4$ may be due to the smallness of ε_f compared to the instrumental resolution.
[12] T. Saitoh *et al.*, Solid State Commun. **95**, 307 (1995).
[13] J.-J. Yeh and I. Lindau, At. Data Nucl. Data Tables **32**, 1 (1985).
[14] F. Gerken, J. Phys. F **13**, 703 (1983).
[15] G. D. Mahan, Phys. Rev. B **11**, 4814 (1975).
[16] F. Iga, Ph.D. thesis, Tohoku University, 1988.
[17] N. E. Bickers, D. L. Cox, and J. W. Wilkins, Phys. Rev. Lett. **54**, 230 (1985).
[18] A. Yanase and H. Harima, Prog. Theor. Phys. Suppl. **108**, 19 (1992).
[19] R. W. Godby, in *Unoccupied Electronic States*, edited by J. C. Fuggle and J. E. Inglesfield (Springer-Verlag, Berlin, 1992), p. 51.
[20] K. Tsutsui *et al.*, Phys. Rev. Lett. **76**, 279 (1996); T. Saso and M. Itoh, Phys. Rev. B **53**, 6877 (1996).
[21] M. M. Steiner, R. C. Albers, and L. J. Sham, Phys. Rev. Lett. **72**, 2923 (1994).
[22] A. Khurana, Phys. Rev. B **40**, 4316 (1989).
[23] C. M. Varma *et al.*, Phys. Rev. Lett. **63**, 1996 (1989).